INL/RPT-24-81003-Revision-0

Summary of Alloy 617 and Alloy 709 Elevated Temperature Crack Growth Test Results from the Planned FY24 Crack Growth Test Activities

September 2024

Michael D McMurtrey, Michael P Heighes

Changing the World's Energy Future

Idaho National Laboratory

INL is a U.S. Department of Energy National Laboratory operated by Battelle Energy Alliance, LLC

INL/RPT-24-81003-Revision-0

Summary of Alloy 617 and Alloy 709 Elevated Temperature Crack Growth Test Results from the Planned FY24 Crack Growth Test Activities

Michael D McMurtrey, Michael P Heighes

September 2024

Idaho National Laboratory
Idaho Falls, Idaho 83415

http://www.inl.gov

Prepared for the
U.S. Department of Energy
Under DOE Idaho Operations Office
Contract DE-AC07-05ID14517

INL/RPT-24-81003

Advanced Reactor Technologies

Summary of Results from Alloy 617 and Alloy 709 Elevated-Temperature Crack-Growth-Test from Planned FY-24 Activities

M3AT-24IN0604051

SEPTEMBER 2024

Michael McMurtrey and Michael Heighes

Idaho National Laboratory

Idaho National Laboratory

Battelle Energy Alliance manages INL for the U.S. Department of Energy's Office of Nuclear Energy

INL/RPT-24-81003

Summary of Results from Alloy 617 and Alloy 709 Elevated-Temperature Crack-Growth-Test from Planned FY-24 Activities

M3AT-24IN0604051

Michael McMurtrey and Michael Heighes
Idaho National Laboratory

September 2024

Idaho National Laboratory
Advanced Reactor Technologies
Idaho Falls, Idaho 83415

http://www.art.inl.gov

Prepared for the
U.S. Department of Energy
Office of Nuclear Energy
Under DOE Idaho Operations Office
Contract DE-AC07-05ID14517

Page intentionally left blank

INL ART Program

Summary of Results from Alloy 617 and Alloy 709 Elevated-Temperature Crack-Growth-Test from Planned FY-24 Activities

INL/RPT-24-81003

September 2024

Technical Reviewer: (Confirmation of mathematical accuracy, and correctness of data and appropriateness of assumptions.)

Ninad Mohale	9/25/2024
Ninad Mohale Technical Reviewer Title	Date

Approved by:

	9/25/2024
Michael E. Davenport ART Project Manager	Date
	9/25/2024
Michelle T. Sharp INL Quality Assurance	Date

Page intentionally left blank

ABSTRACT

This report covers the creep crack growth rate and creep-fatigue crack growth rate testing performed on Alloys 617 and 709 during fiscal year 2024. Crack growth rates over time are reported for several conditions. Challenges in performing the tests were identified, as well as recommendations to improve the testing/analysis for future testing.

Page intentionally left blank

ACKNOWLEDGMENTS

This work was sponsored by the United States (U.S.) Department of Energy (DOE) under Contract No. DE-AC07-05ID14517 with Idaho National Laboratory (INL), which is managed by Battelle Energy Alliance. Programmatic direction was provided by the Office of Nuclear Reactor Deployment of the DOE Office of Nuclear Energy. The authors gratefully acknowledge the support provided by Sue Lesica, the Federal Lead for Advanced Materials of the Advanced Reactor Technologies (ART) Program. The authors thank Gerhard Strydom, the National Technical Director of the ART Gas-Cooled Reactors Campaign. Additionally, the authors thank Ting-Leung Sham, who was the ART Materials Technical Area Lead when this work started, for his substantial support of this project. Lastly, the authors also acknowledge the technical support from Joel Simpson of INL.

Page intentionally left blank

CONTENTS

FIGURES

TABLES

ACRONYMS

ART	Advanced Reactor Technologies (Program)
ASME	American Society of Mechanical Engineers
ASTM	American Society for Testing Materials
BPVC	Boiler and Pressure Vessel Code
CCGR	Creep Crack Growth Rate
C-FCGR	Creep-Fatigue Crack Growth Rate
CGR	Crack Growth Rate
COD	Crack-opening displacement
CT	Compact Tension
DCPD	Direct Current Potential Drop
DOE	Department of Energy
FY	Fiscal Year
INL	Idaho National Laboratory
RIM	Reliability and Integrity Management

Page intentionally left blank

Summary of Results from Alloy 617 and Alloy 709 Elevated-Temperature Crack-Growth-Test from Planned FY-24 Activities

M3AT-24IN0604051

1. INTRODUCTION

The American Society of Mechanical Engineers (ASME) Boiler and Pressure Vessel Code (BPVC) [1] contains rules to maintain nuclear power plants within Section XI. Section XI, Division 2, of the BPVC deals specifically with reliability and integrity management (RIM) programs for nuclear-reactor designs. Materials sections of the codes, such as BPVC, Section III, Division 5, do not include material-degradation management. RIM programs cover the entire life cycle of nuclear power plants and require a combination of monitoring, examination, tests, operation, and maintenance to ensure that each structure, system, and component of the plant operate as expected across their lifetimes. Degradation-mechanism assessment is a part of the RIM program and requires an understanding of the material behavior within the expected environment. Such degradation mechanisms as stress corrosion cracking and radiation embrittlement are concerns for the current fleet of light-water reactors. Advanced reactors operate with very different environments, and their material-degradation mechanisms differ significantly from those of the light-water reactors. Due to high operating temperatures, where time-dependent deformation is active, creep cracking and creep-fatigue cracking are both a potential degradation mechanism of concern for advanced reactors. Other degradation mechanisms of concern to high-temperature gas reactors are listed in Table VII-3.2-1 from Section XI, Division 2, of the ASME BPVC.

To facilitate RIM program development and integration for advanced reactors, crack-growth correlations for creep-crack growth rate (CCGR) and creep-fatigue crack-growth rate (C-FCGR) should be established. This is needed for all Section III, Division 5, materials although this work is currently focused on Alloys 617 and 709. Alloy 617 was recently added to the ASME BPVC [1] through a Code Case in Section III, Division 5, permitting it for use in Class A high-temperature nuclear components [2]. Alloy 709 is being tested to gather data for a Section III, Division 5, Code Case, with a 100,000 hour Code Case expected to be submitted to the ASME BPVC committees soon [3].

Crack-growth rate (CGR) testing relevant to high-temperature nuclear components is included in three American Society for Testing Materials (ASTM) standards: fatigue in ASTM E647 [4], creep in ASTM E1457 [5], and creep-fatigue in ASTM E2760 [6]. A brief description of these testing standards is provided below.

Fatigue CGRs (da/dN, where a refers to the crack length and N the number of fatigue cycles) are compiled as a function of crack-tip stress-intensity factor range (ΔK). The specimen must be thick enough to ensure that buckling does not occur, and the small-scale yielding conditions are maintained for using the linear elastic fracture-mechanics approach. CGRs must be measured during the test because crack size is directly linked to K, which serves as the control variable.

CCGR testing is performed under static or quasi-static loading conditions at elevated temperatures where creep deformation occurs. In this case, creep-crack growth is measured in da/dt (change in crack length over change in time) usually as a function of K, Ct or C* where Ct and C* are the transient and steady-state crack-tip characterizing parameters under the creep condition. The C* parameter is valid only when extensive creeping condition is obtained. The exact choice of parameter to correlate with crack growth depends on the creep properties (creep-ductile or creep-brittle) as well as the specimen geometry. For CCGR testing, loads and temperatures are set, while crack-length history and load-line displacement measurements are continuously recorded during the test.

C-FCGRs seek to capture time-dependent intergranular creep, cycle-dependent transgranular fatigue, and their interactions. The complicated interaction between these two cracking mechanisms is affected by the material, cyclic-loading frequency, and the shape of the load cycle. These parameters simulate the components under in-service conditions. As with CCGRs, the creep portion of the creep-fatigue testing can exhibit creep-ductile or creep-brittle behavior. C-FCGRs are expressed in terms of d*a*/dN expressed in terms of ΔK for creep-brittle materials and da/dt expressed in terms of Ct or C* for creep-ductile materials. The Ct parameter is used to characterize creep CGRs under a wide range of conditions from small-scale to extensive steady-state creep; therefore, it is a time-dependent parameter, and it approaches C* under extensive creep condition. As with C*, continuous monitoring of load line displacement is needed to evaluate Ct, as well as a means for continuous monitoring of the crack length.

All three CGR testing types typically use a compact-tension (CT) type specimen. The importance of each data set is determined by the expected conditions of the component. Where heavy cyclic loading is expected for the component or structure, fatigue CGRs are useful in assessment of cracks (and crack-like defects). Where load/stress is expected to be relatively constant and the component will operate at an elevated temperature, CCGRs are used in the assessment. Where components experience elevated temperature as well as slow-moving cyclic loads, or load where cycles are interrupted with hold times, C-FCGRs are relevant.

This report summarizes the CGR testing performed at Idaho National Laboratory (INL) during fiscal year (FY) 2024 on Alloys 617 and 709. Prior work at INL was reported previously in McMurtrey's 2023 update report, Bass's 2022 report, and Benz and Wright's 2013 conference paper [7,8,9]. In the early work at INL, the effects of material processing (aged, carburized, solution annealed), temperature (650°C and 800°C), environment (air and impure helium), and fatigue loading (frequency and magnitude) were examined using constant K tests. In 2023, the system was modified to include a load-line displacement measurement, and testing began using the combination direct current potential drop (DCPD) and load-line displacement analysis. Prior to 2023, load-line displacement was not measured. This is not a concern for fatigue CGRs, where ΔK was used to evaluate the CGRs; however, for processes involving creep (creep and creep-fatigue CGRs), use of ΔK indicates that the material was creep-brittle. There are concerns that this assumption does not match the actual behavior of Alloy 617, and so this work will continue the work of evaluating Alloy 617 and Alloy 709 while collecting data that allow for analysis using C* and Ct.

2. METHODS

2.1. Materials

The Alloy 617 plate used in this work was produced by ThyssenKrupp Vereinigte Deutsche Metallwerke, Heat 314626. The chemical composition of this heat is provided in Table 1. The significant strengthening mechanisms in Alloy 617 are solid-solution strengthening from Co and Mo as well as precipitation strengthening. The main precipitates that can result in strengthening in Alloy 617 are $M_{23}C_6$, M_6C, and various Ti-containing precipitates. The Alloy 709 plate was produced by Allegheny Technologies Incorporated, Heat CG45192. Alloy 709 is a high-strength stainless steel that is precipitation strengthened by the addition of niobium.

Table 1. Alloy 617, Heat 314626, and Alloy 709, Heat CG45192, compositions (in weight percent).

	Ni	Cr	Co	Mo	Fe	Mn	Al	C	N	Cu	Si	S	Ti	Nb	B	P
617	54.1	22.2	11.6	8.6	1.6	0.1	1.1	0.05	–	0.04	0.1	<0.002	0.4	–	<0.001	–
709	25.0	19.8	0.01	1.5	Bal.	0.9	0.02	0.07	0.15	0.04	0.44	0.001	<0.01	0.18	0.005	0.008

The design of the CT specimen used in this work is shown in Figure 1. The geometry near the mouth of the notch, between the pin loading holes, allows for the use of an extensometer to measure load-line displacement. DCPD wires are welded on to the front face, spanning across the machined mouth/notch from which the crack will initiate and propagate. DCPD is a method of continuously monitoring the crack length based on the potential drop measured as the crack propagates and forces the current to travel further around the crack.

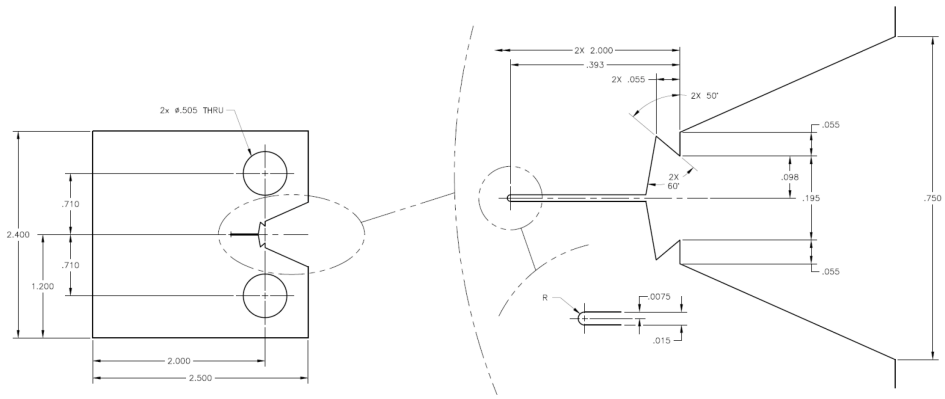

(a)

(b)

Figure 1. (a) Schematic of CT specimens to permit load line displacement measurements, with actual specimens shown in (b).

2.2. Test Frames

Crack-growth testing uses a test frame, furnace, and DCPD system to apply constant stress intensities to the CT specimens, as well as an extensometer when load-line displacement is monitored. The furnace attached to the test frame has a maximum temperature of 1000°C. An Epsilon Model 3548 crack-opening displacement (COD) gauge with 5-mm gauge length and +10-mm range was installed on each of the Instron 8862 load frames to measure load-line displacement. The Instron 8862 electromechanical load frames with 100-kN Dynacell load cells were calibrated and returned to service. DCPD systems, previously used for stress corrosion cracking, that consist of a calibrated Agilent 6611C power supply, calibrated Agilent 34420 nanovoltmeter, Agilent 34970 data-acquisition unit, and INL-manufactured current-switching box were set up on each frame and updated to work with current Windows software. Figure 2 shows the testing setup with both DCPD wires welded on to the specimen, as well as the COD gauge for load-line displacement measurements.

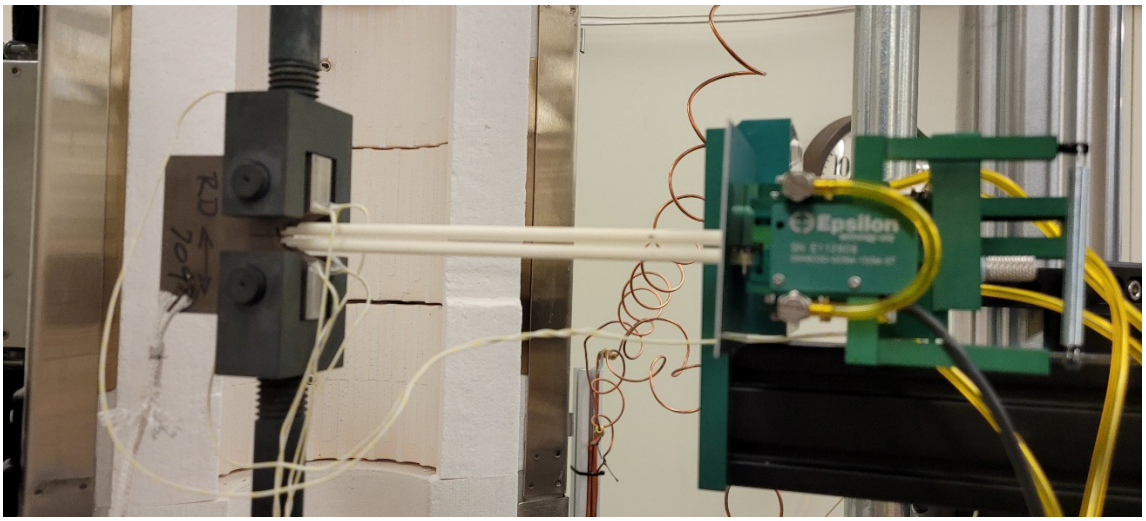

Figure 2. CGR testing setup with DCPD and load line displacement extensometer.

3. RESULTS AND DISCUSSION

Four tests were completed in FY-24, namely Alloy 709, C-FCGR Test 1; Alloy 709, CCGR Test 1; Alloy 709, C-FCGR Test 2; and Alloy 617, CCGR Test 1. All pre-cracks were performed at room temperature. The first test was used to demonstrate the creep-fatigue setup. The test was programmed with the following steps:

1. A room-temperature pre-crack, performed at constant K = 25 MPa√m, R = 0.1, F = 1Hz, Hold = 0s to an a/W = 0.28140
2. A room-temperature pre-crack, performed at constant K=30 MPa√m, R=0.1, F=1Hz, Hold=0s, to an a/W=0.34070
3. Temperature increase to 600°C
4. Creep-fatigue step: cycling started with 1-sec ramp to the maximum load of 2831 lbf and a hold time of 60 sec, followed by a 1-sec ramp down to the minimum load of 283.1 lbf (R = 0.1) for 2500 cycles
5. Fatigue step: cycling with a 1-sec ramp to the maximum load of 2831 lbf, with a hold time of 0 sec, followed by a 1-sec ramp down to a minimum load of 283.1 lbf for 5000 cycles.
6. Repeat Steps 4 and 5 at total of 10 times OR until limits are reached on the load-line displacement extensometer or a/W.

Similar pre-crack procedures were performed on all specimens although later tests went from higher to lower K values, and included a third and final step at a K of 20 MPa√m. The fatigue cycles were intended to act as markers on the fracture surface to validate crack length. However, an issue identified after the test was performed was that the peak load during the creep-fatigue section of the test was 2381 lbf, instead of 2831 lbf, as seen in Figure 3. This results in slow C-FCGR, as compared to CGR during the fatigue cycles that were performed with the correct maximum load. The crack length vs time, relative to the load-line displacement vs time, are shown in Figure 4. While crack growth does occur during the creep-fatigue portion of the test, particularly as the total crack length increases (because this is a load-controlled test, and not stress-intensity controlled), there is concern that the plastic zone ahead of the crack tip during the fatigue cycles may influence the CGR during the creep-fatigue cycles, due to the higher maximum load during the fatigue cycles.

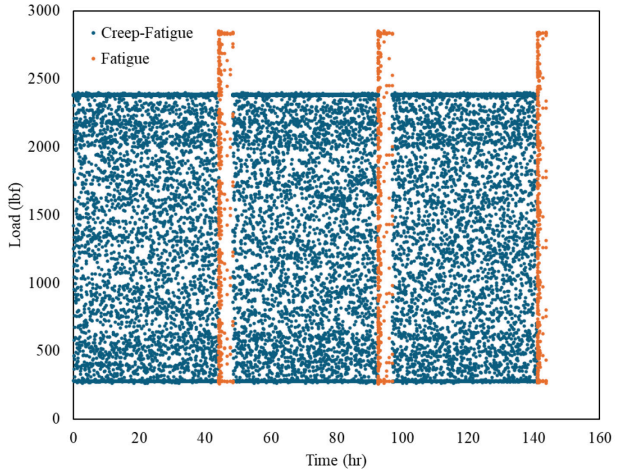

Figure 3. Load vs time for Alloy 709 C-FCGR, Test 1.

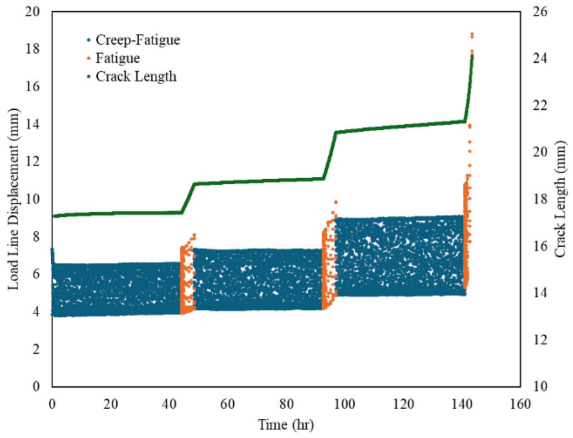

Figure 4. Crack length and load-line displacement versus time of Alloy 709, C-FCGR Test 1.

The DCPD values were checked against measurements taken on the fracture surface (Figure 5), and the results are shown in Table 2. Nine measurements were taken on the fracture surface for each segment, spaced roughly evenly across the width of the specimen; at times the measurement location was moved a little to the side where the fracture surface lines were clearer. In general, the DCPD results match well with the fracture surface measurements. The DCPD data were collected beyond the end of the test, and it was noted that the crack length continued to increase, though these data were cut from the analysis. This is why the final, measured crack length is much greater than the DCPD final measurement.

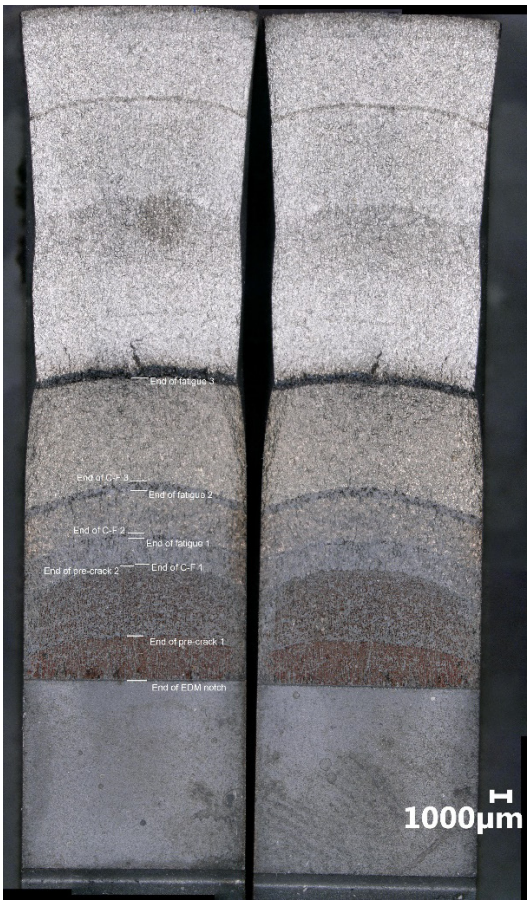

Figure 5. Fracture surface of Alloy-709 specimen from the C-FCGR, Test 1.

Table 2. Alloy 709 C-FCGR Test 1 crack measurements. Measurements made on the fracture surface are an average nine measurements taken from across the width of the specimen.

	DCPD	Fracture surface	
	Crack length (µm)	Average crack length (µm)	Stdev (µm)
Pre-crack 1	1532	2222	389
Pre-crack 2	3018	3705	249
C-F 1	136	93	30
Fatigue 1	1226	1293	492
C-F 2	255	178	32
Fatigue 2	1776	2406	73
C-F 3	632	506	57
Fatigue 3	2684	6171	265

The second test on A709 was a CCGR test performed at 800°C and held with a constant load of 2119 lbf. This test underwent rapid creep deformation, resulting in the load-line displacement extensometer reaching its maximum extension prior to the test specimen's failing. The deformation greatly outpaced the crack growth, resulting in a very blunt crack tip, as shown in Figure 6. While the test was shorter than expected, it did show that the test frame maintained good load control throughout the test (Figure 7), and the load-line displacement and crack-growth rate were collected during the entire load hold (Figure 8) although the extensometer reached its limit around 25 hours, due to the large amount of creep deformation resulting in a large load-line displacement. As in a standard creep test, the load-line displacement saw a rapid increase in creep strain at first (primary creep), followed by a steady-state region (secondary creep). A gradual increase in creep rate (tertiary creep) is just visible prior to the extensometer reaching its limit.

Figure 6. Alloy 709 CCGR, Test 1, CT specimen after termination of the test. Higher-magnification image of the notch tip is shown on the right.

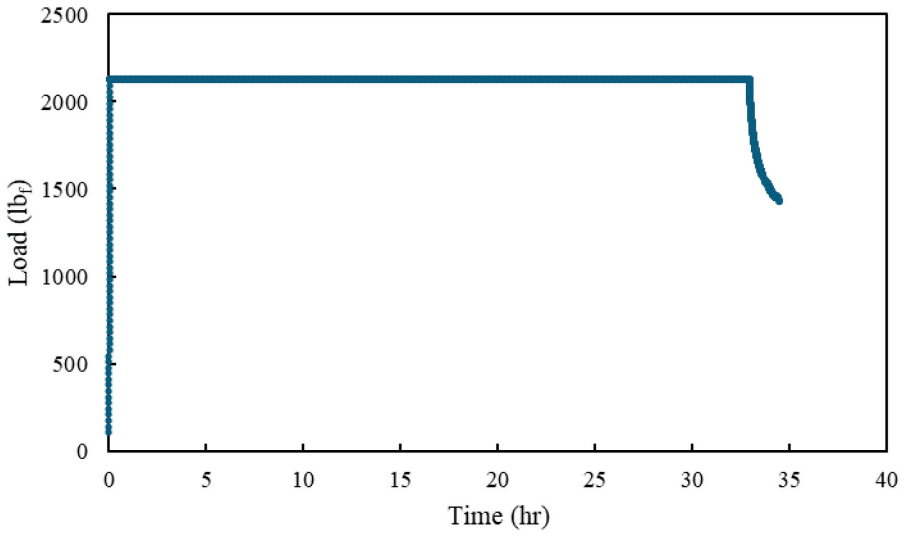

Figure 7. Load over time during the Alloy 709 CCGR Test 1.

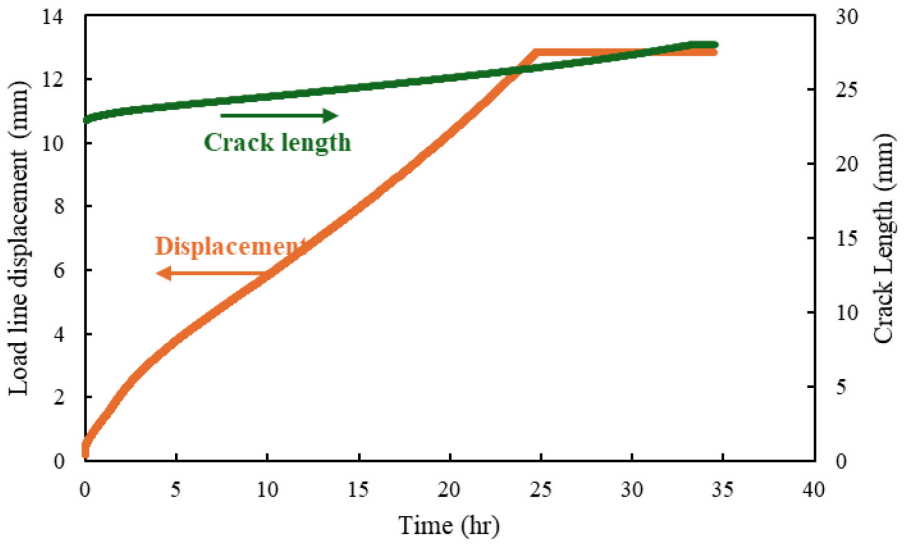

Figure 8. Load-line displacement and crack length over time for Alloy 709, CCGR Test 1.

The creep crack resulted in a more-extreme, non-uniform crack front than has been observed from the fatigue and creep-fatigue cracking. More-severe deformation was also observed at the edges of the specimen around the creep crack. As a result, rather than taking measurements along the width of the specimen that would result in large variations, crack lengths were measured on the fracture surface, as shown in Figure 9, along the center of the thickness. These results are shown in Table 3. While the DCPD underestimates the crack length during the fatigue pre-cracking, it severely overestimates the cracking during the creep step. This is a result of severe deformation occurring during the CCGR step of the test. The creep deformation also resulted in a rapid increase in load-line displacement during the relatively slow crack growth of the test that is seen in Figure 8.

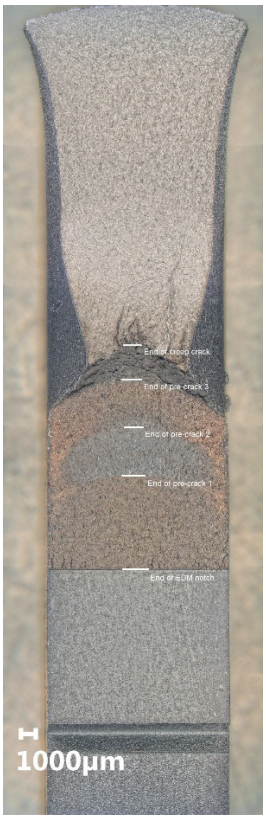

Figure 9. Fracture surface of Alloy 709, CCGR Test 1.

Table 3. Alloy 709, CCGR Test 1, crack measurements. Measurements made on the fracture surface were taken along the center line of the fracture surface.

	Crack length (um)	
	DCPD	Fracture surface
Pre-crack 1	4488	6324
Pre-crack 2	2528	3266
Pre-crack 3	2578	3204
Creep crack	5105	2462

The third and final Alloy 709 test performed in FY-24 was a second C-FCGR test, referred to as Alloy 709, C-FCGR Test 2. It was performed at 954°C and R = 0.1. The initial peak load was 370 lbf, with a 10 minute hold at peak tension each cycle. After approximately 2 mm of crack growth, the creep-fatigue load was increased to a peak load of 740 lbf, with an R = 0.1 and a hold time of 10 minutes at peak tension for each cycle. The load profile is shown in Figure 10. The load-line displacement and crack-length profiles are shown in Figure 11. Note that the test frame recorded data during the 5 hour ramp and soak at temperature prior to the cyclic load beginning to ensure a uniform and steady temperature across the specimen. After a period of rapidly increasing crack length, the crack-growth rate slowed to a steady-state growth rate during the first creep-fatigue segment. Once the peak load was increased, both the load-line displacement and crack length rapidly increased. This rapid failure resulted in a different fracture mode for the final creep-fatigue segment, as seen in the fracture surface in Figure 12. Once again, the high load resulted in significant plastic deformation around the crack and a very uneven crack front, so fracture-surface crack measurements were taken along the center line. The

final results of the DCPD and measurements taken from the fracture surface are shown in Table 4. The DCPD measurements appear similar to the post-test measurements, with the exception of the high-load creep-fatigue segment, where the DCPD heavily underestimates the crack length. This is possibly due to the uneven crack front.

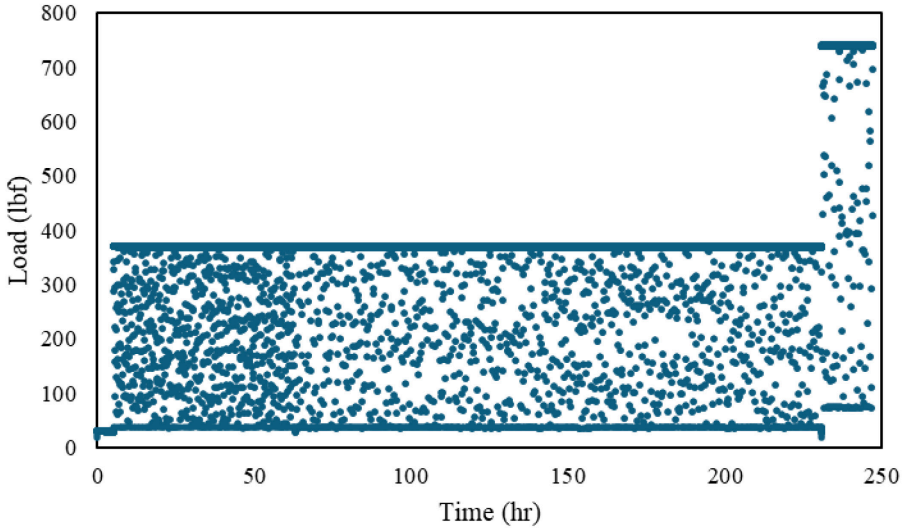

Figure 10. Load vs time for Alloy 709, C-FCGR Test 2.

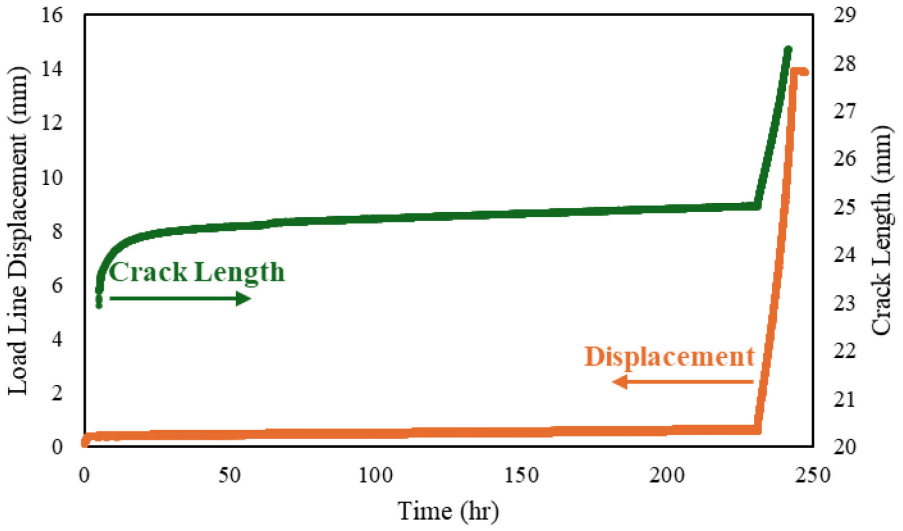

Figure 11. Load-line displacement and crack length vs. time for Alloy 709, C-FCGR Test 2.

Figure 12. Fracture surface of Alloy 709 from C-FCGR Test 2.

Table 4. Alloy 709, C-FCGR Test 2, crack measurements. Measurements made on the fracture surface were taken along the center line of the fracture surface.

	Crack length (um)	
	DCPD	Fracture surface
Pre-crack 1	4933	6870
Pre-crack 2	5049	5152
C-F 1	2079	1370
C-F 2	3113	8185

The Alloy 617 CCGR test was performed in FY 2024 at 850°C and a constant load of 981 lbf (shown in Figure 13, with the inclusion of a 5-hour hold to ramp and soak at temperature). Load-line displacement and crack length are shown in Figure 14. The crack length increases slowly at first, but begins to increase rapidly towards the end of the test as the total crack length increases (resulting in higher stresses at the crack tip). The load-line displacement follows a similar trend at the end of the test, but it is unclear why, at the beginning, it has a sharp knee in the displacement graph at around 90 hours. It appears to be an exaggerated change between primary and secondary creep, but typically would not appear as such a sharp change in deformation rates in typical creep curves.

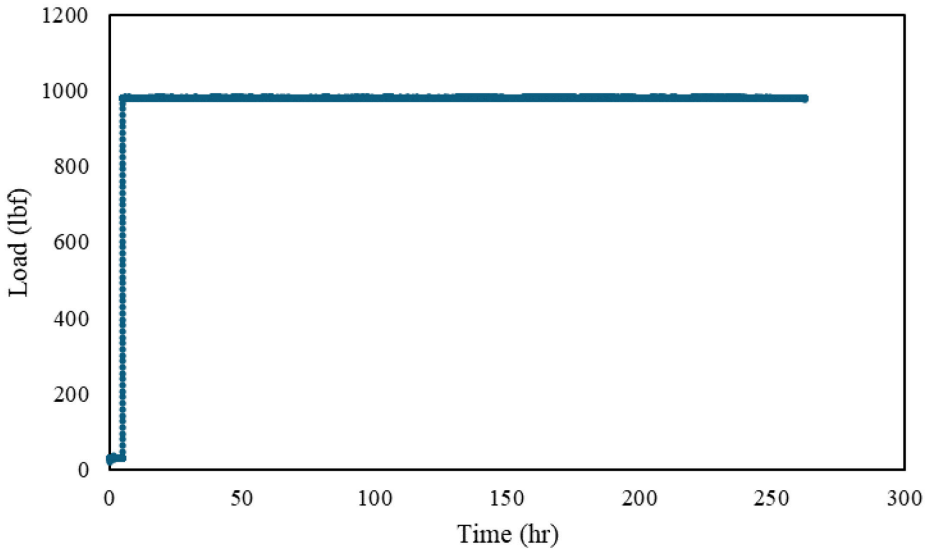

Figure 13. Load vs time for Alloy 617, CCGR Test 1.

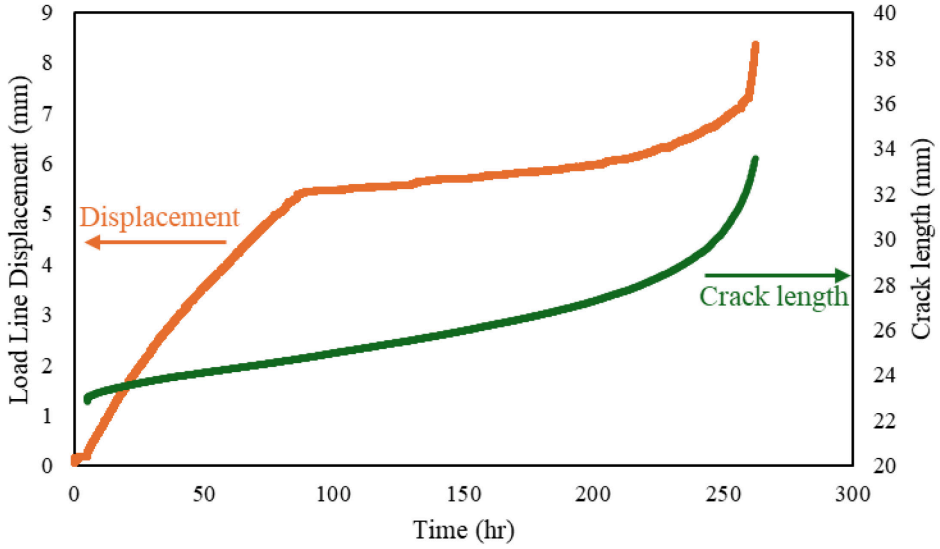

Figure 14. Load-line displacement and crack length vs time for Alloy 617, CCGR Test 1.

The fracture surface for Alloy 617, CCGR Test 1, is shown in Figure 15. Crack lengths for each segment were measured along the center of the specimen and are reported, along with the DCPD measurements, in Table 5. In general, the DCPD and measured crack lengths follow similar trends. In this case, the DCPD consistently underestimates the measured crack length, so a correction factor could be applied to increase the accuracy of the DCPD measurements throughout the test.

Figure 15. Fracture surface for Alloy 617, CCGR Test 1.

Table 5. Alloy 617, CCGR Test 1, crack measurements. Measurements made on the fracture surface were taken along the center line of the fracture surface.

	Crack length (um)	
	DCPD	Fracture surface
Pre-crack 1	5816	8755
Pre-crack 2	3153	4018
Pre-crack 3	639	1470
Creep crack	10713	13851

While there were challenges with some of the tests performed, particularly in cases where high loads resulted in larger-than-expected creep-deformation rates, the testing performed in FY-24 has shown the ability of the system to collected CGR data (both C-FCGR and CCGR). There were issues identified with the setup that will be presented in the final conclusions of this report that, if addressed, would simplify and improve the testing capabilities.

Further analysis is needed on all four specimens to examine the relation between CGR and C* or Ct. This work will be carried over into FY-25, and the analysis will be completed. The relationship between CGR and C* or Ct will provide important information towards a Section XI, Division II, Code Case. The testing performed in this FY does not provide all the data needed for a code case, but it does provide preliminary information. One of the challenges in selecting testing conditions is the lack of available data, requiring that standard creep-rupture data and creep-fatigue data be used to estimate conditions for the CGR testing. To ensure that testing did not progress too slowly, fairly aggressive conditions were chosen for testing this year. The preliminary data in the report will allow for more-refined determination of future test conditions to acquire data across a range of CGRs.

4. CONCLUSIONS

This report shows the results from two CCGR (one Alloy 709, and one Alloy 617), and two C-FCGR (both Alloy 709) tests. A range of loads were tested, resulting in several CGRs. Fairly severe plastic deformation was observed in the tests with high loading (both CCGR and C-FCGR). The large plasticity resulted in increased errors in the DCPD measurements. This will be analyzed with the load-line displacement in the future, which should help separate the deformation from the cracking effects in the DCPD data. Ongoing work that will carry over into FY-25 will finish the C*/Ct analysis and provide the relation between them and CGRs. These relationships will help support the development of a future ASME BPVC Section XI, Division 2, Code Case.

Several challenges and issues were noted during this testing. It is noted that the standard for CCGR testing [5] recommends that direct load-test frames be used for this testing. While the electromechanical frames used for all testing within this report were able to consistently hold a constant load, this may become more challenging for longer tests. It is noted that CCGR tests are often greater than 1000 hours, which is longer than the relatively short tests performed within this work. It is also noted that the extensometer style used resulted in a loss of load-line displacement data for the CCGR testing due to the larger amount of deformation occurring, in addition to the crack lengths' increasing, which resulted in a larger crack-mouth-opening displacement. An extensometer with a longer operating range will increase the reliability of the data collection during CCGR testing. Finally, the analysis was severely hampered and made more challenging by the use a of a custom built DCPD system used along with Instron's Bluehill software to control frame and collect all other instrumentation data. These systems could not communicate with each other and computer time stamps were needed to connect the DCPD data to other data collected during the test—specifically, the load-line displacement. A unified setup that controls the test frame along with the DCPD hardware would greatly simplify the setup and analysis.

5. REFERENCES

1. ASME. 2023. "Boiler and Pressure Vessel Code (BPVC)." American Society of Mechanical Engineers, New York, NY.
2. ASME. 2023. "Boiler and Pressure Vessel Code (BPVC)." Code Case N-898, American Society of Mechanical Engineers, New York, NY.
3. Sham, T.-L., Y. Wang, R. Bass, X. Zhang. 2022. "A709 Qualification Plan Update and Mechanical Properties Data Assessment." INL/RPT-22-67641, Idaho National Laboratory. https://www.osti.gov/servlets/purl/1906516.
4. ASTM. 2023. "Standard Test Method for Measurement of Fatigue Crack Growth Rates." ASTM E647-23a, ASTM International, West Conshohocken, PA.
5. ASTM. 2022. "Standard Test Method for Measurement of Creep Crack Growth Times in Metals." ASTM E1457-19e1, ASTM International, West Conshohocken. PA.

6. ASTM. 2020. “Standard Test Method for Creep-Fatigue Crack Growth Testing.” ASTM E2760-19e1, ASTM International, West Conshohocken, PA.
7. McMurtrey, M., M. Heighes, and C. Gibson. 2023. “Results of FY 2023 Alloy 617 and Alloy 709 High-Temperature Crack-Growth Testing.” INL/RPT-23-74791, Idaho National Laboratory.
8. Bass, J. 2022. “Results of Initial Alloy 617 High Temperature Crack Growth Testing.” INL/RPT-22-69322, Rev. 0, Idaho National Laboratory. https://inldigitallibrary.inl.gov/sites/sti/sti/Sort_63641.pdf.
9. Benz, J. and R. Wright. 2013. “Fatigue and Creep Crack Propagation behaviour of Alloy 617in the Annealed and Aged Conditions.” INL/CON-13-30214, in proceedings of the Third International Workshop on Structural Materials for Innovative Nuclear Systems, Idaho Falls, ID. https://www.osti.gov/servlets/purl/1111504.